

# AN EFFICIENT IMPLEMENTATION FOR BLOCK-IFDMA

Tobias Frank\*, Anja Klein\*, Elena Costa\*\*

\* Technische Universität Darmstadt, Communications Engineering Lab, Merckstr. 25, 64283, Darmstadt, Germany

\*\* Nokia Siemens Networks GmbH & Co. KG, Werinherstr. 91, 81541 München, Germany

Email: t.frank@nt.tu-darmstadt.de, elena.costa@nsn.com

## ABSTRACT

Recently, a new multiple access (MA) scheme denoted Block-Interleaved Frequency Division Multiple Access (B-IFDMA) has been proposed which can be regarded as a generalization of Interleaved Frequency Division Multiple Access (IFDMA). Compared to IFDMA, B-IFDMA provides higher flexibility, increased robustness to carrier frequency offsets and additional power savings at the mobile terminal at the expense of increased envelope fluctuations and higher complexity. In this paper, different variants of B-IFDMA are presented and their properties are discussed. Moreover, new algorithms for a low complexity implementation of B-IFDMA providing low envelope fluctuations are introduced. The complexity of B-IFDMA is shown to be lower than for OFDMA. New performance results for coded transmission over a mobile radio channel are given.

## I. INTRODUCTION

Currently, research on B3G/4G mobile radio systems is ongoing worldwide. The choice of the MA scheme has a great impact on the characteristics of the system. In order to provide packet based transmission of multi-media services at acceptable costs, desired properties of the MA scheme are, e.g., good performance, high flexibility, low complexity, robustness to real world effects and provision of low cost mobile terminals with low power consumption.

For scenarios where reliable channel state information at the transmitter is not available, the exploitation of diversity is the preferred strategy for provision of good performance [1]. In this context, especially in the uplink, DFT precoded OFDMA with interleaved subcarrier allocation spread over the total available bandwidth, also called IFDMA, cf. [2, 3], has been receiving wide interest and is currently considered as promising candidate MA scheme, e.g., in 3GPP LTE [4] or in the European Union research project WINNER [5]. Spreading of the subcarriers over the total bandwidth leads to high frequency diversity. DFT precoding provides a considerable reduction of the envelope fluctuations of the transmit signal compared to non-precoded OFDMA. Thus, for IFDMA the utilization of low cost power amplifiers at the user terminal (UT) is possible and a lower power back-off compared to non-precoded OFDMA is required. The lower power back-off results in lower power consumption due to a power efficient use of the amplifier [6]. Moreover, IFDMA provides low complexity and high flexibility in terms of different data rates [3, 7]. However, IFDMA suffers from high pilot symbol overhead for channel estimation [8] and high sensitivity to carrier frequency offsets [9].

Recently, a new MA scheme based on DFT precoded OFDMA with interleaved assignment of subcarrier blocks, cf. Fig. 1, has been proposed [1]. The scheme is referred to as B-IFDMA and can be regarded as a generalization of IFDMA. Due to the equidistant assignment of blocks of subcarriers instead of single subcarriers, compared to IFDMA the robustness to frequency offsets is increased and the pilot symbol overhead is reduced since for pilot assisted channel estimation interpolation in frequency direction within a block becomes possible.

Moreover, B-IFDMA supports the efficient use of a micro-sleep mode resulting in additional power savings at the UT compared to IFDMA [1, 10]. The advantages of B-IFDMA are basically obtained at the expense of a higher complexity for signal processing and increased envelope fluctuations of the transmit signal compared to IFDMA, resulting in undesired additional costs at the UT.

In this paper, two different variants of B-IFDMA are presented and their properties are discussed. Moreover, new algorithms for a low complexity implementation of B-IFDMA modulation and demodulation providing low envelope fluctuations are proposed. The complexity of B-IFDMA is analyzed and compared to that of other MA schemes. Moreover, new performance results for coded B-IFDMA transmission over a mobile radio channel are given.

The paper is organized as follows: In Section II, a system model for the different variants of B-IFDMA is given. After a discussion of the properties of B-IFDMA in Section III, in Section IV the novel algorithms for the implementation of B-IFDMA are introduced. The complexity is analyzed in Section V and the performance results are given in Section VI.

## II. SYSTEM MODEL

In this section, a system model for B-IFDMA is derived as special case of DFT-precoded OFDMA. In the following, all signals are represented by their discrete time equivalents in the complex baseband. Further on,  $(\cdot)^T$  denotes the transpose,  $(\cdot)^{-1}$  the inverse and  $(\cdot)^H$  the Hermitian of a vector or a matrix, respectively.

### A. DFT precoded OFDMA Modulation

For a system with  $K$  users with user index  $k$ ,  $k = 0, \dots, K - 1$ , let

$$\mathbf{d}^{(k)} = (d_0^{(k)}, \dots, d_{Q-1}^{(k)})^T \quad (1)$$

denote a block of  $Q$  data symbols  $d_q^{(k)}$ ,  $q = 0, \dots, Q - 1$ , of user  $k$  at symbol rate  $1/T_s$ . The data symbols  $d_q^{(k)}$  may be taken from the alphabet of a bit mapping scheme like Phase Shift Keying (PSK) or Quadrature Amplitude Modulation (QAM), applied after Forward Error Correction (FEC) coding and interleaving. Further on, let  $\mathbf{F}_N^H$  denote the matrix representation of an  $N$ -point Inverse DFT (IDFT), where  $N = K \cdot Q$  denotes the number of subcarriers available in the system. The assignment of the data symbols  $d_q^{(k)}$  to a user specific set of  $Q$  subcarriers is described by an  $N \times Q$  subcarrier allocation matrix  $\mathbf{M}^{(k)}$ . Thus, in general, a DFT-precoded OFDMA signal of user  $k$  can be described by vector  $\mathbf{x}^{(k)} = (x_0^{(k)}, \dots, x_{N-1}^{(k)})^T$ , with  $N$  elements  $x_n^{(k)}$ ,  $n = 0, \dots, N - 1$ , at sample rate  $1/T_c = K/T_s$  given by

$$\mathbf{x}^{(k)} = \mathbf{F}_N^H \cdot \mathbf{M}^{(k)} \cdot \mathbf{F}_Q \cdot \mathbf{d}^{(k)}, \quad (2)$$

where  $\mathbf{F}_Q$  denotes a  $Q$ -point DFT matrix for precoding. Before transmission over a multi-path channel, a Cyclic Prefix (CP) [11] is applied to the signal from Eq. (2).

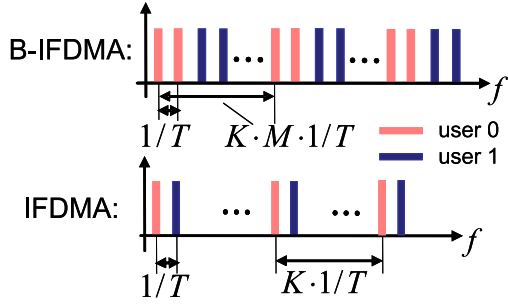


Figure 1: Subcarrier allocation for B-IFDMA and IFDMA. IFDMA can be regarded as B-IFDMA with  $M = 1$ .

### B. B-IFDMA Modulation

In the following, the system models for two possible variants of B-IFDMA are derived. The first one, referred to as Joint-DFT B-IFDMA, is based on the application of one DFT over all subcarriers assigned to a specific user  $k$ , the second one, referred to as Added-Signal B-IFDMA, is based on the assignment of multiple IFDMA signals to one user. The two variants result in two different signals with different properties. In the sequel, let  $M$  denote the number of subcarriers per block and let  $L$  denote the number of blocks assigned to a specific user  $k$ , with  $Q = M \cdot L$ .

*Joint-DFT B-IFDMA:* Let  $\mathbf{M}_B^{(k)}$  denote a block interleaved subcarrier allocation matrix with elements  $M_B^{(k)}(n, q)$  in the  $n$ -th row,  $n = 0, \dots, N-1$ , and  $q$ -th column,  $q = l \cdot M + m$ ;  $l = 0, \dots, L-1$ ;  $m = 0, \dots, M-1$  defined as

$$M_B^{(k)}(n, q) = \begin{cases} 1 & n = l \cdot \frac{N}{L} + m + kM \\ 0 & \text{else} \end{cases} \quad (3)$$

Thus, a possible transmit signal for B-IFDMA is given by setting  $\mathbf{M}^{(k)}$  in Eq. (2) to  $\mathbf{M}^{(k)} = \mathbf{M}_B^{(k)}$ .

*Added-Signal B-IFDMA:* In order to get the signal model for Added-Signal B-IFDMA, it is assumed that  $M$  IFDMA signals, each with  $L$  subcarriers are superimposed and assigned to user  $k$ . The  $M$  IFDMA signals assigned to user  $k$  are mutually shifted by one subcarrier bandwidth. The resulting Added-Signal B-IFDMA signal can be described as follows: Let  $\bar{\mathbf{d}}^{(m,k)}$  denote the  $m$ -th  $L$  elementary subblock of  $\mathbf{d}^{(k)}$  with elements  $\bar{d}_l^{(m,k)} = d_{mL+l}^{(k)}$ ;  $l = 0, \dots, L-1$ . The  $N \times L$  subcarrier allocation matrix  $\mathbf{M}_I^{(m,k)}$  of the  $m$ -th IFDMA signal assigned to user  $k$  is defined by its elements

$$M_I^{(m,k)}(n, l) = \begin{cases} 1 & n = l \cdot \frac{N}{L} + m + kM \\ 0 & \text{else} \end{cases} \quad (4)$$

Thus, the Added-Signal B-IFDMA signal for user  $k$  can be obtained by

$$\mathbf{x}^{(k)} = \sum_{m=0}^{M-1} \mathbf{F}_N^H \cdot \mathbf{M}_I^{(m,k)} \cdot \mathbf{F}_L \cdot \bar{\mathbf{d}}^{(m,k)}, \quad (5)$$

where  $\mathbf{F}_L$  denotes an  $L \times L$  DFT matrix.

Let  $\mathbf{I}_L$  denote an  $L \times L$  identity matrix and let  $\mathbf{R}$  denote an  $N \times L$  repetition matrix  $\mathbf{R}$  obtained by stacking  $K$  identity matrices according to

$$\mathbf{R} = (\mathbf{I}_L, \dots, \mathbf{I}_L)^T. \quad (6)$$

Further on, let

$$\Phi^{(k)} = \text{diag}(\phi_0^{(k)}, \dots, \phi_{N-1}^{(k)}), \quad (7)$$

define a user dependent  $N \times N$  diagonal matrix with diagonal elements  $\phi_n^{(k)} = 1/\sqrt{K} \cdot e^{j \frac{2\pi}{N} \cdot n(kM+m)}$ , where  $n = 0, \dots, N-1$  and  $m = 0, \dots, M-1$ . It is shown in [3] that the term  $\mathbf{F}_N^H \cdot \mathbf{M}_I^{(m,k)} \cdot \mathbf{F}_L$  from Eq. (5) can be reformulated as

$$\mathbf{F}_N^H \cdot \mathbf{M}_I^{(m,k)} \cdot \mathbf{F}_L = \Phi \cdot \mathbf{R}^{(k)}. \quad (8)$$

The expression on the right in Eq. (8) represents a  $K$ -fold compression in time and a subsequent  $K$ -fold repetition, cf. matrix  $\mathbf{R}$ , followed by a phase rotation according to matrix  $\Phi^{(k)}$ . Thus, with Eq. (8) follows that the Added-Signal B-IFDMA signal from Eq. (5) can be efficiently generated in time domain by using a sum of IFDMA signals generated by compression and repetition of the data block  $\mathbf{d}^{(k)}$  of user  $k$  and subsequent user specific phase rotation, cf. [2, 3].

### C. B-IFDMA Demodulation

In the following, the demodulators for the two variants of B-IFDMA from Section II-B are described.

*Joint-DFT B-IFDMA:* For demodulation of Joint-DFT B-IFDMA, the operations from Eq. (2) have to be performed in reversed order. In a first step, after removal of the CP, an  $N$ -point DFT has to be applied. Subsequently, a subcarrier demapping has to be performed. Finally, the DFT precoding is neutralized by application of an IDFT. Let  $(\cdot)^\dagger$  denote the pseudo-inverse of a matrix. The demodulated B-IFDMA signal  $\rho^{(k)} = (\rho_0^{(k)}, \dots, \rho_{Q-1}^{(k)})^T$  of user  $k$  is given by

$$\rho^{(k)} = \mathbf{F}_Q^H \cdot \mathbf{M}_B^{(k)\dagger} \cdot \mathbf{F}_N \cdot \mathbf{r}, \quad (9)$$

where  $\mathbf{F}_Q^H$  and  $\mathbf{F}_N$  denote a  $Q$ -point IDFT matrix and an  $N$ -point DFT matrix, respectively.

*Added-Signal B-IFDMA:* Let  $\bar{\rho}^{(m,k)} = (\bar{\rho}_0^{(m,k)}, \dots, \bar{\rho}_{L-1}^{(m,k)})^T$  denote the  $m$ -th subblock of the demodulated B-IFDMA signal  $\rho^{(k)}$  with elements  $\bar{\rho}_l^{(m,k)} = \rho_{mL+l}^{(k)}$ . The Added-Signal B-IFDMA signal is demodulated subblock by subblock. The subblocks  $\bar{\rho}^{(m,k)}$  are given by

$$\bar{\rho}^{(m,k)} = \mathbf{F}_L^H \cdot \mathbf{M}_I^{(m,k)\dagger} \cdot \mathbf{F}_N \cdot \mathbf{r}; \quad m = 0, \dots, M-1 \quad (10)$$

where  $\mathbf{F}_L^H$  denotes an  $L$ -point IDFT matrix.

## III. PROPERTIES OF B-IFDMA

In this section, the properties of B-IFDMA are briefly analyzed. Due to the block interleaved subcarrier allocation spread over the total available bandwidth, B-IFDMA provides high frequency diversity gains. At the same time, low potential multi-user scheduling gains are provided, because the exploitation of frequency diversity lowers the channel variations between different users. Thus, similar to IFDMA, B-IFDMA is an appropriate scheme for scenarios where channel state information at the transmitter side is not available or not reliable, e.g., due to high user velocity, and where, hence, adaptive transmission and adaptive multi-user scheduling is not possible.

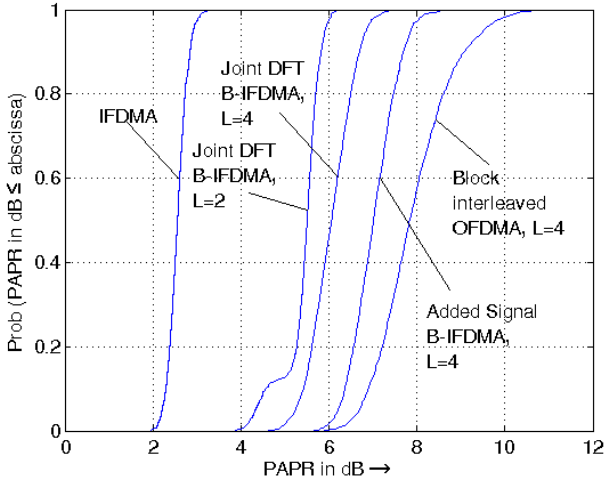


Figure 2: PAPR for the transmit signal of different multiple access schemes for  $Q=128$  subcarriers per user and  $N=1024$  available in the system.

Compared to IFDMA, B-IFDMA requires a lower overhead for pilot transmission for channel estimation. Indeed, in contrast to IFDMA, by using pilot assisted channel estimation, interpolation in frequency domain between the pilots within a block of subcarriers becomes possible for B-IFDMA. Thus, combined with Time-Division Multiple Access (TDMA), the assignment of short TDMA blocks to a user is possible with low channel estimation overhead. The use of short TDMA blocks enables micro-sleep modes that result in significant power savings at the UTs [1]. Further on, in the uplink, B-IFDMA provides a higher robustness to frequency offsets compared to IFDMA for uplink transmission. The robustness to frequency offsets increases with increasing number of subcarriers per block.

In Fig. 2 the Peak-to-Average Power Ratio (PAPR) for Joint-DFT and Added-Signal B-IFDMA is given and compared to the PAPR of OFDMA and IFDMA schemes. From Fig. 2 it can be deduced that the advantages of B-IFDMA compared to IFDMA are obtained at the expense of an increased Peak-to-Average Power Ratio (PAPR) of the transmit signal. However, compared to OFDMA the PAPR of B-IFDMA is significantly lower. The trade-off between PAPR reduction and pilot overhead increase for a lower number  $M$  of subcarriers per block is subject of further study. A comparison of Joint-DFT B-IFDMA and Added-Signal B-IFDMA shows that the implementation with joint DFT provides a significantly lower PAPR.

For the same number  $Q$  of subcarriers assigned to a user, the computational effort for B-IFDMA at the transmitter and at the receiver is higher than for IFDMA. Considering the computational complexity, Added-Signal B-IFDMA is preferable compared to Joint-DFT B-IFDMA because Added-Signal B-IFDMA benefits from the very efficient signal generation scheme in time domain for IFDMA, cf. II-B.

Since Joint-DFT provides a significantly lower PAPR compared to Added-Signal B-IFDMA, algorithms providing lower computational complexity for the implementation of Joint-DFT B-IFDMA are desirable.

#### IV. EFFICIENT IMPLEMENTATION

Since also Joint-DFT B-IFDMA provides a regular subcarrier assignment, the computational complexity for Joint-DFT B-IFDMA modulation and demodulation can be further reduced

compared to Eqs. (2) and (9). A reduction of the computational complexity is especially desirable for the modulator in the uplink and for the demodulator in the downlink, which are both situated in the UT. In the following, novel algorithms for an efficient implementation of Joint-DFT B-IFDMA modulation and demodulation are presented.

#### A. Modulation

Let

$$D_p^{(k)} = \frac{1}{\sqrt{Q}} \sum_{q=0}^{Q-1} d_q^{(k)} \cdot e^{-j \frac{2\pi}{Q} pq}; \quad p = 0, \dots, Q-1 \quad (11)$$

denote the  $Q$  elements of the DFT of the data symbols  $d_q^{(k)}$ . The  $N$  elements  $x_n^{(k)}$  of the transmit signal from Eq. (2) using the block interleaved subcarrier allocation matrix  $M_B^{(k)}$ , cf. Eq. (3), can be rewritten as follows:

$$x_n^{(k)} = \frac{1}{\sqrt{N}} \sum_{\eta=0}^{N-1} \tilde{D}_\eta^{(k)} \cdot e^{j \frac{2\pi}{N} \eta n}; \quad n = 0, \dots, N-1, \quad (12)$$

with

$$\tilde{D}_\eta^{(k)} = \begin{cases} D_{lM+m}^{(k)} & \text{for } \eta = l \cdot \frac{N}{L} + m + kM \\ 0 & \text{else} \end{cases} \quad (13)$$

Eq. (12) represents the IDFT for OFDM modulation and Eq. (13) represents block interleaved subcarrier mapping, cf. Eq. (3). Insertion of Eq. (13) and Eq. (11) into Eq. (12) results in

$$x_n^{(k)} = \frac{1}{\sqrt{QN}} \sum_{m=0}^{M-1} e^{j \frac{2\pi}{N} n(kM+m)} \sum_{q=0}^{Q-1} d_q^{(k)} e^{-j \frac{2\pi}{Q} qm} \sum_{l=0}^{L-1} e^{j \frac{2\pi}{L} l(n-q)}, \quad (14)$$

where

$$\sum_{l=0}^{L-1} e^{j \frac{2\pi}{L} l(n-q)} = \begin{cases} L & \text{for } q = n + \mu L \\ 0 & \text{else} \end{cases}, \quad (15)$$

for  $\mu = 0, \dots, M-1$ . Insertion of Eq. (15) in Eq. (14) leads to

$$x_n^{(k)} = \frac{L}{\sqrt{QN}} \sum_{\mu=0}^{M-1} d_{(n+\mu L) \bmod Q}^{(k)} e^{j \frac{2\pi}{N} nkM} \sum_{m=0}^{M-1} e^{-j 2\pi m (\frac{n}{Q} - \frac{n}{N} + \frac{\mu}{M})}. \quad (16)$$

Defining

$$\Theta_n^{(\mu,k)} = \frac{L}{\sqrt{QN}} e^{j \frac{2\pi}{N} nkM} \sum_{m=0}^{M-1} e^{-j 2\pi m (\frac{n}{Q} - \frac{n}{N} + \frac{\mu}{M})}, \quad (17)$$

Eq. (16) reduces to

$$x_n^{(k)} = \sum_{\mu=0}^{M-1} d_{(n+\mu L) \bmod Q}^{(k)} \cdot \Theta_n^{(\mu,k)}. \quad (18)$$

Eq. (18) can be implemented as depicted in Fig. 3. In a first step, the data block  $\mathbf{d}^{(k)}$  of user  $k$  is compressed in time by factor  $K$  and subsequently repeated  $K$ -times resulting in  $K \cdot Q = N$  elements. The  $N$  elements are, element by element, multiplied with the elements  $\Theta_n^{(\mu,k)}$  of  $M$  different user specific sequences  $\Theta_0^{(\mu,k)}, \dots, \Theta_{N-1}^{(\mu,k)}$ ;  $\mu = 0, \dots, M-1$ . The sequences  $\Theta_0^{(\mu,k)}, \dots, \Theta_{N-1}^{(\mu,k)}$  are independent on the data symbol vector  $\mathbf{d}^{(k)}$  and, thus, can be calculated offline. Finally, the resulting  $M$  different sequences resulting from multiplication of the cyclically shifted elements  $d_{(n+\mu L) \bmod Q}^{(k)}$  of the compressed and repeated data block with  $\Theta_n^{(\mu,k)}$  are summed up.

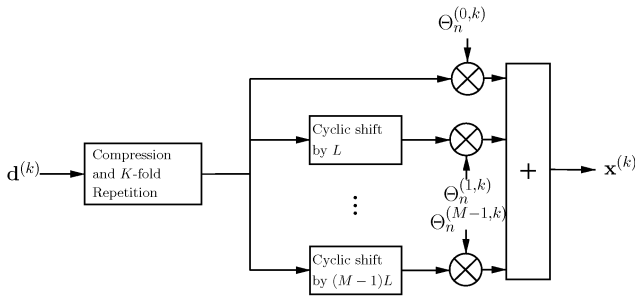


Figure 3: Low complexity implementation for Joint-DFT B-IFDMA modulation

### B. Demodulation

Let

$$R_n = \frac{1}{\sqrt{N}} \sum_{\eta=0}^{N-1} r_\eta \cdot e^{-j\frac{2\pi}{N}\eta n}, \quad n = 0, \dots, N-1, \quad (19)$$

denote the elements of the DFT of the received signal vector  $\mathbf{r}^{(k)}$  at the receiver. The  $Q$  elements  $\hat{\rho}_q^{(k)}$  of the B-IFDMA signal after demodulation can be obtained by

$$\hat{\rho}_q^{(k)} = \frac{1}{\sqrt{Q}} \sum_{p=0}^{Q-1} \tilde{R}_p^{(k)} \cdot e^{j\frac{2\pi}{Q}pq}, \quad p = 0, \dots, Q-1 \quad (20)$$

with

$$\tilde{R}_p^{(k)} = \begin{cases} R_{lN/L+m+kM} & \text{for } p = lM + m \\ 0 & \text{else} \end{cases}. \quad (21)$$

Eq. (20) represents the IDFT for compensating the DFT precoding and Eq. (21) represents block interleaved subcarrier demapping, cf. Eq. (3). Insertion of Eq. (21) and Eq. (19) into Eq. (20) results in

$$\hat{\rho}_q^{(k)} = \frac{1}{\sqrt{QN}} \sum_{m=0}^{M-1} \sum_{\eta=0}^{N-1} r_\eta e^{j\frac{2\pi}{Q}mq} e^{-j\frac{2\pi}{N}\eta kM} \cdot e^{-j\frac{2\pi}{N}\eta m} \sum_{l=0}^{L-1} e^{j\frac{2\pi}{L}l(q-\eta)}, \quad (22)$$

where

$$\sum_{l=0}^{L-1} e^{j\frac{2\pi}{L}l(\eta-q)} = \begin{cases} L & \text{for } \eta = q + \mu L \\ 0 & \text{else} \end{cases}, \quad (23)$$

$\nu = 0, \dots, N/L - 1$ . Insertion of Eq. (23) in Eq. (22) leads to

$$\begin{aligned} \hat{\rho}_q^{(k)} &= \frac{L}{\sqrt{QN}} \sum_{m=0}^{M-1} \sum_{\nu=0}^{N/L-1} r_{(q+\nu L)\text{mod}N} e^{j\frac{2\pi}{Q}mq} e^{-j\frac{2\pi}{N}kM(q+\nu L)} \cdot e^{-j\frac{2\pi}{N}(q+\nu L)m} \\ &= \frac{L}{\sqrt{QN}} \sum_{\nu=0}^{N/L-1} r_{(q+\nu L)\text{mod}N} e^{-j\frac{2\pi}{N}kM(q+\nu L)} \cdot \sum_{m=0}^{M-1} e^{j\frac{2\pi}{Q}m((q+\nu L)-\frac{2\pi}{N}m(q+\nu L))} e^{j\frac{2\pi}{M}(\nu \text{mod} M)m} \end{aligned} \quad (24)$$

Defining

$$\Psi_n^{(\nu, k)} = \frac{L}{\sqrt{QN}} \left( \Theta_n^{(-\nu \text{mod} M, k)} \right)^*; \quad n = (q + \nu L)\text{mod}N, \quad (25)$$

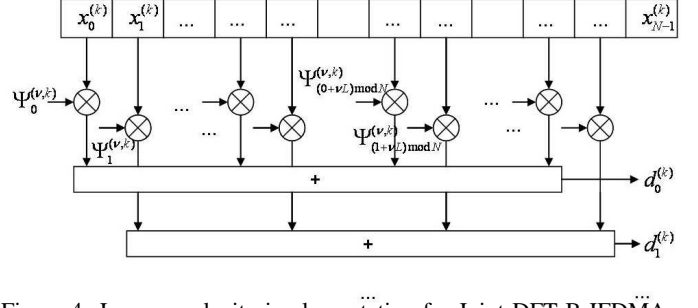


Figure 4: Low complexity implementation for Joint-DFT B-IFDMA demodulation

Table 1: Computational complexity for the uplink transmitter and the downlink receiver in terms of complex multiplications per UT.

Joint-DFT B-IFDMA, conventional	$N/2 \cdot \log_2 N + Q/2 \cdot \log_2 Q$
Joint-DFT B-IFDMA, efficient	$N \cdot M$
Added-Signal B-IFDMA	$N \cdot M$
IFDMA	$N$
OFDMA	$N/2 \cdot \log_2 N$

$\nu = 0, \dots, N/L - 1, q = 0, \dots, Q - 1$ , Eq. (24) can be simplified to

$$\hat{\rho}_q^{(k)} = \sum_{\nu=0}^{N/L-1} r_{(q+\nu L)\text{mod}N} \cdot \Psi_{(q+\nu L)\text{mod}N}^{(\nu, k)}. \quad (26)$$

Eq. (26) can be implemented as depicted in Fig. 4. For each element  $\hat{\rho}_q^{(k)}$  of the received signal after demodulation, the  $N/L$  elements  $r_{(q+\nu L)\text{mod}N}$  from the received signal are multiplied with  $\Psi_{(q+\nu L)\text{mod}N}^{(\nu, k)}$  and summed up. Note that, similar as for the modulation algorithm, the coefficients  $\Psi_{(q+\nu L)\text{mod}N}^{(\nu, k)}$  at the demodulator can be calculated offline.

### V. COMPUTATIONAL COMPLEXITY

In this section, the computational complexity of the efficient implementation for Joint-DFT B-IFDMA from Section IV is compared to the complexity of the conventional implementation for Joint-DFT B-IFDMA according to Eq. (2) and Eq. (3) and with the complexity of Added-Signal B-IFDMA, cf. Eq. (4) and Eq. (8). Further on, the computational complexity is compared to the complexity of IFDMA and OFDMA.

In the following, it is assumed that  $N, Q, M$  and  $L$  are chosen as powers of 2 in order to make the utilization of the FFT

Table 2: Computational complexity for the uplink transmitter and the downlink receiver in terms of complex multiplications per UT.

	B-IFDMA			IFDMA	OFDMA
	Joint DFT Efficient	Conventional	Added Signal		
$N = 2048; Q = 256$					
M=2	4096	12288	4096	2048	11264
M=4	8192	12288	8192	2048	11264
$N = 4096; Q = 256$					
M=2	8192	25600	8192	4096	24576
M=4	16384	25600	16384	4096	24576
$N = 4096; Q = 1024$					
M=2	8192	29696	8192	4096	24576
M=4	16384	29696	16384	4096	24576

Table 3: Simulation parameters

Carrier frequency	3.7 GHz	Decoder	BCJR
Bandwidth	40 MHz	Equalizer	MMSE FDE
No. of subcarriers	1024	Interleaving	Random
Modulation	QPSK	Interl. depth	0.35 ms
Code	Convol.	Guard interval	3.2 $\mu$ s
Code rate	1/2	Channel	WINNER [12]
Constraint length	6	Scenario	Urban, 50 km/h

algorithm for the DFT and IDFT operations possible. However, note that for the efficient implementation according to Section IV, this assumption is not required.

From Eq. (18) and Eq. (26) follows that the required numbers of complex multiplications for modulation and for demodulation are equal. The required number of complex multiplications for modulation and demodulation, respectively, are given in Table 1. Note that for IFDMA demodulation an efficient implementation, cf. [2] can be used, which is already considered in Table 1. The computational effort using the efficient implementation for Joint-DFT B-IFDMA is the same as for the implementation of B-IFDMA using a sum of IFDMA signals. Consequently, compared to IFDMA, the computational complexity is higher. An example for the values for different numbers  $N$  of subcarriers in the system and different numbers  $Q$  of subcarriers per user are given in Table 2. From Tables 1 and 2 follows that for the given parameters, the efficient implementation of Joint-DFT B-IFDMA provides up to factor 3 lower computational effort compared to the implementation according to Eq. (2). The advantage of the efficient implementation increases with increasing the number  $N$  of subcarriers in the system, with increasing data rates, i.e., increasing the number  $Q$  of subcarriers assigned to a user and decreasing the number  $M$  of subcarriers per block. Note that with decreasing the number  $M$  of subcarriers per block not only the computational complexity decreases, but also the PAPR reduces. However, the lower  $M$ , the higher the pilot symbol overhead as well as the sensitivity to frequency offsets.

## VI. PERFORMANCE RESULTS

In Fig. 5 the coded performance for B-IFDMA transmission over a mobile radio channel with parameters according to Table 3 is given. As already mentioned in Section III, similar to IFDMA, also B-IFDMA provides high frequency diversity. As expected, for coded transmission, Added-Signal and Joint-DFT B-IFDMA show the same performance. Compared to B-IFDMA, the performance of IFDMA is slightly better, because for IFDMA the  $Q$  subcarriers are fading independently whereas for B-IFDMA within each block the fading of  $M = 4$  carriers is correlated.

## VII. CONCLUSION

In this paper, Joint-DFT B-IFDMA and Added-Signal B-IFDMA have been analyzed. A low complexity implementation for Joint-DFT B-IFDMA has been presented and shown to provide a significant complexity reduction especially for high data rates. With the proposed implementation, Joint-DFT B-IFDMA is advantageous compared to Added-Signal B-IFDMA since Joint-DFT B-IFDMA provides lower PAPR at the same performance and complexity as Added-Signal B-IFDMA. Providing lower pilot symbol overhead for channel estimation and higher robustness to frequency offsets compared to IFDMA, Joint-DFT B-IFDMA is a promising alternative to IFDMA es-

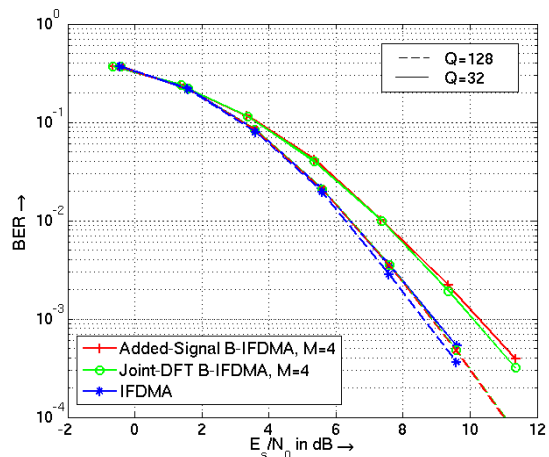


Figure 5: Coded performance for B-IFDMA and IFDMA for different Data rates.

pecially for non-adaptive transmission in the uplink of future mobile radio systems.

## ACKNOWLEDGMENT

This work was performed in the framework of the IST project IST-4-027756 WINNER II, which is partly funded by the European Union. The authors would like to acknowledge the contributions of their colleagues in WINNER II, although the views expressed are those of the authors and do not necessarily represent the project.

## REFERENCES

- [1] WINNER, "The WINNER II Air Interface: Refined multiple access concepts," Tech. Rep. D4.6.1, IST-4-027756 WINNER II, November 2006.
- [2] U. Sorger, I. De Broeck, and M. Schnell, "IFDMA - A New Spread-Spectrum Multiple-Access Scheme," in *Proc. ICC'98*, Atlanta, Georgia, USA, June 1998, pp. 1013–1017.
- [3] T. Frank, A. Klein, E. Costa, and E. Schulz, "IFDMA - A Promising Multiple Access Scheme for Future Mobile Radio Systems," in *Proc. PIMRC 2005*, Berlin, Germany, Sep. 2005.
- [4] 3GPP TSG RAN, "Physical Layer Aspects for Evolved UTRA (Release 7)," TR 25.814v1.5.0, 3rd Generation Partnership Project, Technical Specification Group, Sophia-Antipolis, France, 2006.
- [5] WINNER, *Wireless World Initiative New Radio*, www.ist-winner.org.
- [6] E. Costa and S. Pupolin, "M-QAM-OFDM System Performance in the Presence of a Nonlinear Power Amplifier and Phase Noise," *IEEE Transactions on Communications*, vol. 50, pp. 462–472, March 2002.
- [7] T. Frank, A. Klein, E. Costa, and E. Schulz, "Interleaved Orthogonal Frequency Division Multiple Access with Variable Data Rates," in *Proc. International OFDM Workshop 2005*, Hamburg, Germany, Aug./Sep. 2005, pp. 179–183.
- [8] A. Sohl, T. Frank, and A. Klein, "Channel Estimation for DFT precoded OFDMA with blockwise and interleaved subcarrier allocation," in *Proc. International OFDM Workshop 2006*, Hamburg, Germany, August 2006.
- [9] R. Dinis, C. T. Lam, and D. Falconer, "Carrier Synchronization Requirements for CDMA Systems with Frequency-Domain Orthogonal Signature Sequences," in *Proc. of ISSSTA2004*, Sydney, Australia, Aug./Sep. 2004, pp. 821–825.
- [10] T. Svensson et al., "B-IFDMA - A Power Efficient Multiple Access Scheme for Non-frequency-adaptive Transmission," in *Proc. of 16th Mobile & Wireless Communications Summit*, Budapest, Hungary, July 2007.
- [11] Z. Wang and G.B. Giannakis, "Wireless Multicarrier Communications," *IEEE Signal Processing Magazine*, pp. 29–48, May 2000.
- [12] WINNER, "Final Report on Link Level and System Level Channel Models," Tech. Rep. D5.4 v. 1.4, WINNER-2003-507581, November 2005.